Diffusion Tensor Imaging (DTI) at Multiple Diffusion Times in Mammary Fibroglandular Tissue and Cancerous Lesions

Gene Young Cho[1,2], Ana Paula Klautau Leite[1], Steven Baete[1], Daniel K Sodickson[1], Sungheon Kim[1], Linda Moy[3], and Eric E Sigmund[1]

[1]Radiology - Center for Biomedical Imaging, New York University School of Medicine, New York, NY, United States, [2]Sackler Institute of Graduate Biomedical Sciences, New York University School of Medicine, New York, NY, United States, [3]Radiology - Cancer Institute, New York University School of Medicine, New York, NY, United States

Introduction: Diffusion-weighted imaging (DWI) is a versatile imaging tool to examine tissue microstructure, including comparing healthy tissue to cancerous lesions. DWI is sensitive to restricted water diffusion in cancer as restrictions arise from high cellularity which reduces extracellular space. Diffusion tensor imaging (DTI) [1] provides additional structural sensitivity by measuring directional variance of the diffusion behavior, and quantifying diffusion anisotropy. Oriented tissue types exhibit anisotropic diffusion behavior. This can be distinguished from abnormal, heterogeneous lesion tissue, which often display isotropic behavior. Recently, DTI has been used to probe mammary fibrograndular tissue (FGT) and breast lesions, showing the anisotropic behavior found in the ducts and its disruption in cancerous tissue [2-5]. In this work, we explore the variation of diffusion times as a contrast variable since longer diffusion times increase apparent restriction as more barriers are encountered. This effect may enhance structural sensitivity and provide better distinction between mammary FGT and lesion tissue [6]. We have collected DTI data at two different diffusion times in patients with and without lesions and also compared DTI with typical clinical assessments of breast FGT tissue and lesion malignancy.

Method: In this study, 19 patients (11 lesion free screening patients; 8 patients with lesions and 9 total lesions: 8 invasive ductal carcinomas (IDC) and 1 ductal carcinoma in situ (DCIS)) underwent routine MR breast imaging along with an IRB-approved, HIPAA-compliant DTI protocol in a Siemens 3T Tim Trio scanner using a 7-channel breast coil (Invivo Corp). The DTI protocol collected axial images using a stimulated echo (STEAM) sequence with echo-planar imaging (EPI) readout and SPAIR fat suppression (TR/TE - 7700/40, 192 x 132 matrix, 1.3x1.3x3 mm resolution, 6 directions, 3 averages) at two different b values (0 and 500 s/mm^2). Scans were performed at two diffusion times (t_D - 30 and 520 ms) by varying the stimulated echo mixing time. Total acquisition time was ~5.5 mins. The DTI data was processed offline (Igor Pro, Wavemetrics Inc) to generate maps of mean diffusivity (MD), fractional anisotropy (FA), and diffusion eigenvalues (λ_1, λ_2, λ_3) incorporating encoding matrices (b-matrices) provided by the vendor software including the effects of all imaging, spoiler, and diffusion gradients. Regions of interest (ROIs) were manually drawn in contiguous regions of FGT on all slices to calculate mean values of the DTI parameters individually in both left and right breasts. ROIs were also drawn and DTI metrics derived from known lesions, guided by contrast-enhanced MRI and MD maps. Signal-to-noise ratio (SNR) was estimated for b = 500 s/mm^2 and for both diffusion times by dividing the mean signal intensity in FGT by the standard deviation of signal intensity in a region outside the body. Clinical markers were also collected: mammographic density; background parenchymal enhancement (BPE), and amount of FGT seen on MRI; for patients with lesions: BIRADS score, estrogen receptor (ER), progesterone receptor (PR), Her2/neu, and Ki-67 expression. Group statistical comparisons with a paired Student's t-test were performed for each parameter comparing values from the two diffusion times as well as between normal FGT and lesion. Relative contrast was computed for each subject and metric as ratio of the difference in values in FGT and lesion to their average, expressed as a percentage. Pearson correlations were performed between all DTI metrics, individually at each diffusion time and the clinical markers, and group comparisons were also performed for DTI metrics in binary clinical variables (e.g. ER+ vs. ER-) using Student's t-test. Fiber tractography (MedINRIA) was performed on the t_D = 520 ms dataset from selected subjects with a significant amount of contiguous fibroglandular tissue. Seed points were placed throughout the breast DWI volume and a minimum FA threshold of 0.2 was used. Tracks were visualized with direction color-encoded (red=left/right, green=anterior/posterior, blue=superior/inferior) tube streamlines.

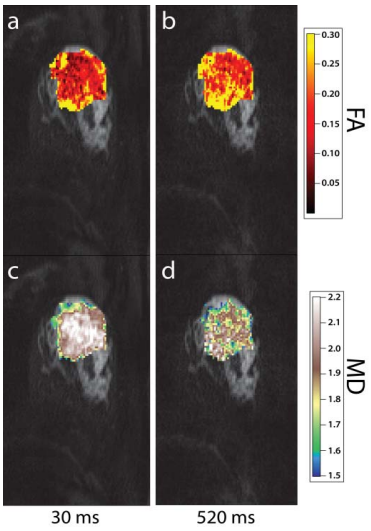

Figure 1. DTI parametric maps in normal FGT (a),(b): Fractional anisotropy (FA) maps; (c),(d): Mean diffusivity (MD) (in μm^2/ms) maps at two diffusion times.

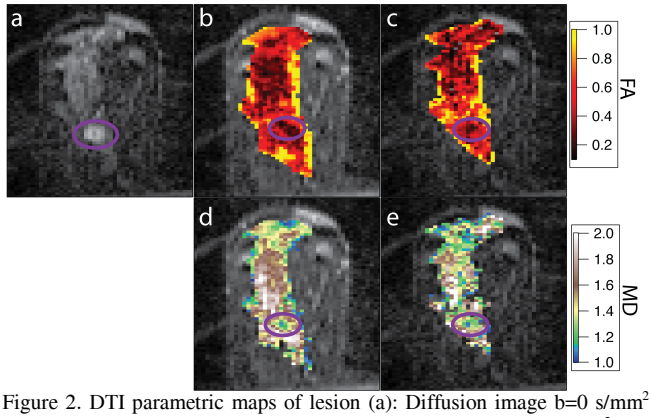

Figure 2. DTI parametric maps of lesion (a): Diffusion image b=0 s/mm^2 (b),(c): Fractional anisotropy maps; (d),(e): Mean diffusivity (in μm^2/ms) maps at two diffusion times. Note: lesion is highlighted by purple circle.

Results: SNR values for all cases were sufficient (SNR>20) to neglect the influence of noise in the comparison of diffusion contrast as a function of diffusion time. Fig. 1 shows parametric maps of the MD and FA of a subject with abundant FGT at two different diffusion times. FA values increase and MD values decrease with longer diffusion times. Fig. 2 illustrates an example of a patient with IDC, in which the lesion possesses lower MD and lower FA than surrounding FGT. Table 1 shows diffusion metrics for all subjects and diffusion times for lesions and FGT. In FGT, significant differences were observed ($p<0.05$) between the two diffusion times for both FA and λ_3. Significant differences were also seen for all parameters between FGT and lesion DTI measurements at each diffusion time (higher FA; lower MD, λ_1, λ_2, λ_3). Relative contrast between lesion and FGT is higher for all parameters at larger diffusion time. No significant correlations were seen between clinical data and DTI. Fig. 3 illustrates an example of a tractography result from a subject in a breast volume, showing the expected predominant anterior-posterior orientation of the ductal tree.

Table 1	Normal FGT		Lesion		Relative Differences (%)	
	30 ms	520 ms	30 ms	520 ms	30 ms	520 ms
FA	0.23±0.081 *†	0.31±0.11‡	0.34±0.16†	0.38±0.20‡	41.21±30.85	30.82±25.01
MD (μm^2/ms)	1.77±0.48†	1.59±0.41‡	1.11±0.55†	0.93±0.52‡	34.54±29.05	41.39±26.35
λ_1 (μm^2/ms)	2.14±0.53†	2.11±0.47‡	1.58±0.67†	1.48±0.71‡	28.66±28.65	33.32±27.31
λ_2 (μm^2/ms)	1..72±0.49†	1.59±0.41‡	1.08±0.56†	0.92±0.52‡	35.33±29.28	42.11±27.52
λ_3 (μm^2/ms)	1.34±0.47*†	1.11±0.38‡	0.66±0.46 †	0.45±0.44‡	48.28±26.93	58.94±31.27

*denotes significant finding between diffusion times †‡denotes significant findings between normal FGT and Lesion at same diffusion times

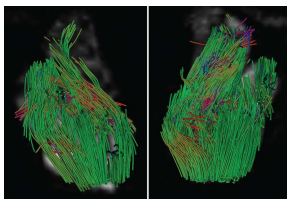

Fig 3. Breast tractography from subject at t_D = 520 ms with anterior-posterior directionality in ductal tree

Discussion: The changes in FGT DTI parameters (decreased MD/λ_2/λ_3 and increased FA) as diffusion lengths ($l_d \approx (2*\lambda_1*t_d)^{0.5}$) increases from 11 μm and 47 μm is consistent with increased restriction to transverse diffusion, possibly from confinement in oriented ductal tubules. Lesion diffusivities decreased at long times, possibly due to restrictive cellularity. The result of these changes is higher lesion conspicuity via DTI at longer diffusion times as shown in the relative contrast improvement. Regarding comparison with clinical markers, FA of FGT and of lesions showed promising trends ($p\sim0.06$) of correlation between mammographic density/BPE and MD, λ_1, λ_2, λ_3. These trends bear further study, but could indicate macromolecular influences such as dense collagen contributing to ductal anisotropy. In summary, we have found that increased sensitivity to restriction at higher diffusion time changes MR diffusion metrics in normal and cancerous breast tissue and may increase lesion detection.

References:1. Baltzer, P.A., et al., EurRadiol,2011. **21**(1). **2.**Eyal, E., et al., IR,2012. **47**(5). **3.**Partridge, S.C., et al., MRI,2010. **28**(3). **4.**Partridge, S.C., et al.,JMRI, 2010. **31**(2). **5.**Tagliafico, A., et al., RadMed,2012. **6.**Sen, P.N., ConcMR,2004. **23A**(1).